ZANCO Journal of Pure and Applied Sciences
The official scientific journal of Salahaddin University-Erbil
https://zancojournals.su.edu.krd/index.php/JPAS

ISSN (print):2218-0230**, ISSN (online):** 2412-3986**, DOI: http://dx.doi.org/10.21271/zjpas**

RESEARCH PAPER

Stability Investigation of Contiguous Replacement Piles

Hangaw Najm Ahmed [1], Yousif Ismael Mawlood [1]

[1]Department of Civil Engineering, College of Engineering, Salahaddin University-Erbil, Kurdistan Region, Iraq.

A B S T R A C T:

Urbanization leads to increase lands cost which resulted in the construction of high towering vertically toward the sky and use underground for construction. Foundations of these structures need deep excavation. Anti-slide piles are a suitable option for excavation stability, which involves bored cast-in-place piles constructed along the line of the excavation as a retaining structure using closely bored piles. There is a gap between two individual piles. For this purpose, an experimental study on anti-sliding piles was investigated, For further investigation of contiguous pile system, and their behavior under different soil types, and to study the effect of embedment ratio and relative density on lateral displacement of the contiguous pile.

Physical scale model tests were performed to investigate the effect of the fine-grained soils, coarse-grained soils, various embedment ratios, and density on the lateral displacement. The test results showed that lean clay (CL) soil is more stable to resist lateral displacement induced by inter-particle cohesion. Increasing the embedding ratio significantly reduced the lateral displacement, and with increasing backfill density of sandy soil for high embedment ratio the lateral displacement noticeably decreased, while for the low value of embedment ratio the lateral displacement increase with increase backfill density.

KEY WORDS: Anti-slide pile, physical model test, embedment depth, lateral displacement.
DOI: http://dx.doi.org/10.21271/ZJPAS.35.SpA.2
ZJPAS (2023) , 35(SpA);11-25 .

1.INTRODUCTION :

Increased land costs as a result of urbanization have led to the construction of high-rise buildings that rise vertically into the sky and the use of underground construction. Excavation is needed for the construction of basements or foundations for high-rise buildings and underground structures. (Ou, 2014). During excavation on the same site may encounter various types of soil from soft clay to hard rocks. Therefore some types of soil lead to instability problems. One of the dangerous types of soil is sandy soil after a vertical cut when it is stood alone for a period of time (Godavarthi et al., 2011). A contiguous pile wall involves bored cast-in-place piles constructed along the line of the retaining wall, retaining structures using closely bored piles. There is a gap between two individual piles (Godavarthi et al., 2011). The distance size is influenced by the site's proportions as well as the real ground condition, but is generally between 50 to 150 mm, as shown in **Figure 1**.

Contiguous pile walls are best used in cohesive soils with a groundwater table below the excavation level. The wall is made up of discrete column piles that are normally put at a short gap for soft soils or at a larger spacing for stiff soils. (Clayton et al., 2014). Water does not remain in contiguous bored piles. If the wall must retain water, the area between the piles can be grouted before excavation., Alternatively, the shotcrete-facing wall could be added. (Money et al., 1996). During excavation, soil gaps between adjacent piles are left and exposed. Large and small diameter bored cast-in-place piles are commonly used to build a contiguous pile wall for temporary or permanent constructions like deep basements, cut-and-cover tunnels, tunnel shaft stations, underpasses. To achieve acceptable ground movements, bracings of a contiguous wall are also required. The main advantages of contiguous pile walls are their cost-effectiveness, as unconnected piles require less concrete and low-cost augers can

* **Corresponding Author:**
Hangaw Najm Ahmed
E-mail: hangaw.ahmed@su.edu.krd
Article History:
Received: 17/11/2022
Accepted: 07/02/2023
Published: 01/11/2023

be used to drill holes for these piles, providing another alternative for a cost-effective retaining wall. (Keawsawasvong et al., 2017). The spacing ratio between adjacent piles is one critical component that influences the short-term performance of contiguous pile walls. Despite the fact that soil gaps in adjacent pile walls are freely exposed, they are stable due to a self-supporting mechanism caused by an arching effect that occurs in soil gaps between two adjacent piles working against lateral earth pressure behind them. The most critical components of this design problem are the predictions of the undrained limiting pressure behind soil gaps and the lateral force acting on a pile in a contiguous pile wall in respect to this factor(Keawsawasvong et al., 2017).

The selection of embedment depth of piles depend on the depth of the wall, conditions of the ground, types of soil, strength of soil, and bulk density whether or not the piles would be concentrically loaded. Due to the gaps between singular piles, the contiguous piled walls cannot be used as an everlasting wall; they can, however, be turned into a permanent solution by using a structural facing wall. An appropriate capping beam should be mounted on top of the piles for uniformity and grade repairs (Akrawi and Ahmed, 2019).

For anti-slide piles to exert their holding ability, the soil arching effect is essential. Pile space is related to the soil arching behind piles and is an important aspect of pile design [7]. The landslide thrust could be transferred to the pile body by soil arching, which would then transport the stress underground. Pile space has been shown to be one of the most important influencing variables on soil arching (Li et al., 2013). A large pile gap can result in invalid soil arching between piles and may cause slippage. If the pile space is too small, the material may be wasted (Liu et al., 2020).

Hassiotis et al. (1997) suggested a method of design for pile systems to reach the required factor of safety, based on the theory of plasticity. Cai and Ugai (2011), Broms (1964), and Rathod et al. (2018) concluded that dimensionless (unitless) lengths control the anti-sliding pile's behavior. While several researchers concluded that piles stiffness also has the greatest role in the stabilizing system. For example, piles' elastic modulus has a large effect on the p–y characteristics (Li et al., 2018). Shooshpasha and Amirdehi (2015) concluded that increasing bending stiffness of a pile causes to increase in the factor of safety of the slope. Several researchers are performing a numerical study on anti-sliding piles like Poulos (1995) suggested an approach for the design of piles for retaining slopes. Muraro et al. (2014) performed a study on a single pile when affected by lateral soil movement by using three-dimensional finite element analyses. Kahyaoglu et al. (2012) for the free head passive pile groups which are in cohesionless soils evaluated the mechanisms of the load transformation by using three-dimensional finite element analyses and indicated that by decreasing the pile spacing the load transfer decreases proportionally. Kanagasabai et al. (2011) performed a study on a single pile which embedded into a stable stratum to stabilize a slipping mass of soil. Kourkoulis et al. (2012) progressed a hybrid method for designing anti-sliding piles, by a combination of rigorous three-dimensional finite elements and widely accepted analytical techniques.

Aimin et al. (2006) and Xing et al. (2013) indicate some mechanical parameters impact soil arching like Poisson's ratio, soil cohesion, and some others, they concluded that Poisson's ratio is inversely proportional to the soil arching, while soil cohesion has a proportional effect on the soil arching, and indicate that other mechanical parameters of soil have no obvious impact. Liu et al. (2011) performed a study on the soil arching effect on the spacing of double-row piles and concluded that if the pile width is less than row spacing by four times causes to loss of effect of soil arching between piles, and indicated that if the row spacing equal to 2.0-2.5 times the diameter of the pile the arching effect of soil is greatest.

The participation of various related parameters makes determining the lateral load capacity of piles a complicated problem.(Johari and Nakhaee, 2013). The elastic limit displacement has a mean value of 5% to 6% of the pile diameter, and its coefficient of variation is approximately 40% to 60% (Shirato et al., 2009). For determining the typical lateral displacement, **Table 1** shows the methods for achieving active and passive states in various soils (Das, 2010)

Short and long pile foundations are the two types of pile foundations. Laterally loaded piles that are short or "rigid" have the depth that smaller than the required to anchor the toe against rotations as shown in **Figure 2(a)** (Chik et al., 2009). When ultimate loads occur, the soil usually fails first. Alternatively, long piles provide more embedment establishing the pile toe, which makes it fixed as indicated in **Figure 2(b)** (Chik et al., 2009).

According to its stiffness and the lateral resistance provided by the soil, piles are categorized as long or short. If the L/D (where L = length, D = diameter of the pile) is greater than 20, the pile is considered long (Broms and division, 1964).
According to (Prakash and Sharma, 1991), there are two failure modes to define the allowed lateral loads on piles: 1-The ultimate lateral load (with the factor of safety). 2- Maximum allowable lateral load corresponding with acceptable lateral displacement. The design lateral load of the pile is chosen from the smaller of the two values above. The following are some methods for estimating the maximum lateral load of a pile foundation:
1. Methods for calculating ultimate lateral load:
a. Hansen (1961)
b. Broms (1964a) c. Meyerhof et al (1981)
2. (p-y curve) method for calculating allowable displacement at working lateral load, like using API RP 2GEO Design Method (RP, 2011).
Due to lack of the experimental work on the contiguous pile, in this study prepared the physical model for the contiguous pile to investigate and study the two types of soil, clayey soil, and sandy soil. And various embedment depths.

Table 1: Typical Values of ΔL_a/H and ΔL_p/H (Das, 2010)

Soil type	ΔL_a/H	ΔL_p/H
Loose sand	0.001–0.002	0.01
Dense sand	0.0005–0.001	0.005
Soft clay	0.02	0.04
Stiff clay	0.01	0.02

ΔL_a &ΔL_p are horizontal displacements for active and passive states respectively, and H is the height of the wall.

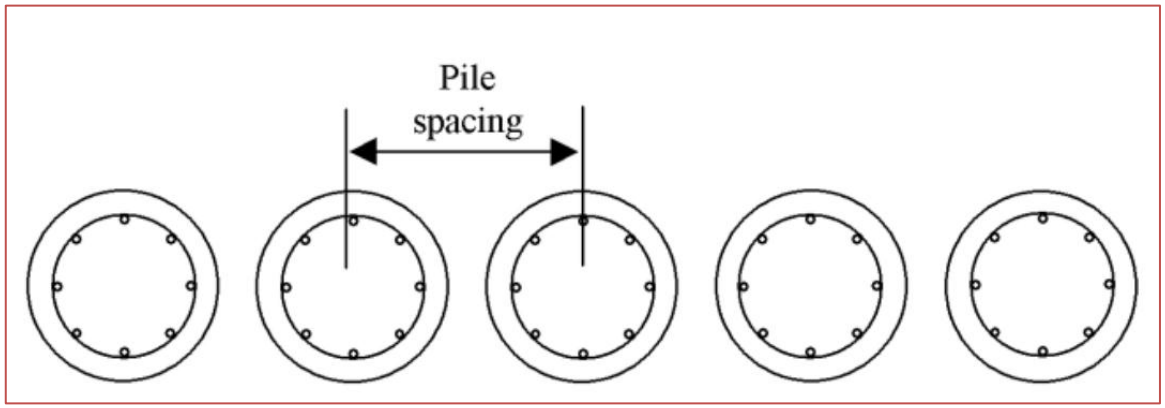

Figure 1: Contiguous pile wall.

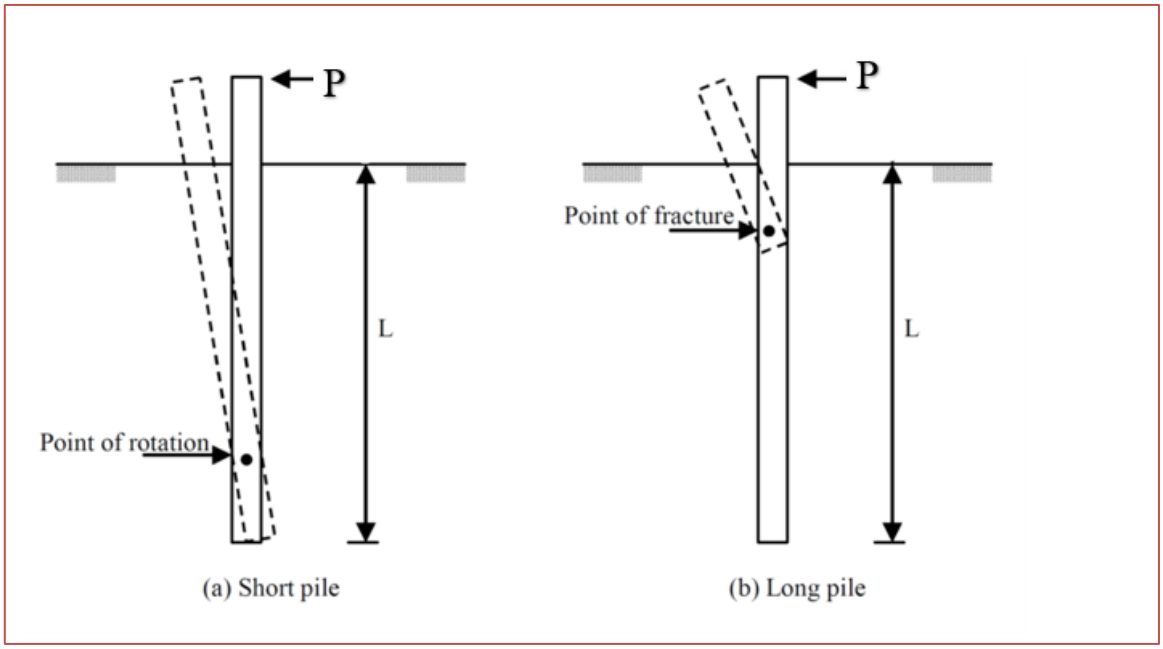

Figure 2: Failure modes of short and long piles under lateral loads

2. MATERIALS AND METHODS

2.1 Model preparation

An experimental physical model must match a prototype in behavior (Tang et al., 2014). The physical model should be dynamically the same as the actual prototype in terms of its physical parameters, geometry, initial state, and boundary conditions.

The results of the model testing differ from those of the prototype. A well-designed physical model retaining the broad interpretation can deliberately set out to probe rival conjectures. Poorly designed physical modelling is mere data gathering. If the models to be tested are not understood or recognized then it is unlikely that the correct data will be assembled: the physical modelling is then stuck in the *prediction*/*observation*(Wood, 2017). To correlate both responses, a set of scaling relations is required. The model test should replicate the prototype's actual situation, according to the physical scaling law.

For the experimental model select one prototype project as a case study in Erbil City as shown in **Figure 3**, then produced by scale 1:50. The prototype is excavated for 18m, and pile length, pile diameter, and spacing between adjacent piles are 36 m, 1.0 m, and 0.2 m respectively. The corresponding parameters for the model after scaling are 720 mm, 20 mm, and 4 mm, respectively. Based on the work of (Liu et al., 2018) and (Ye et al., 2020), selecting the model's dimension which is 900 mm in length, 400 mm in width, and 850 mm in height as shown in **Figure 4**.

Used Galvanized pipes with outer and inner diameters of 19 mm and 12.7 mm, respectively as a model pile, and covered by mortar cement to attain the same friction between soil and pile as a prototype, and reach the 20 mm diameters of the pile.

Figure 3: prototype project.

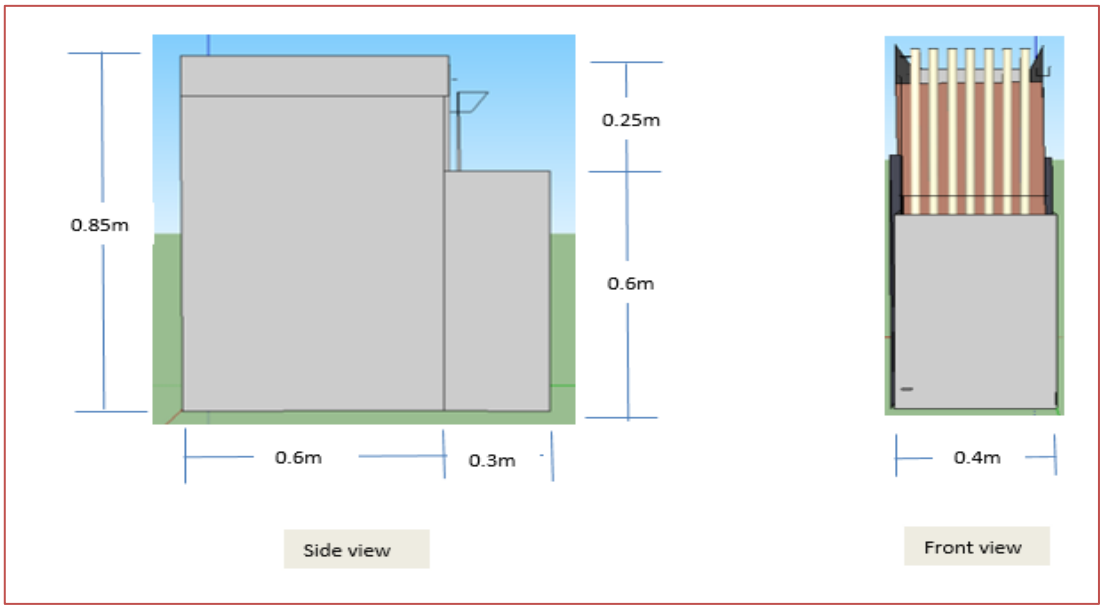

Figure 4: Experimental model dimensions.

2.2 Soil types

Using two types of soil, fine- and coarse-grained soils, the fine-grained soil that was brought from the in-situ soil of the prototype as shown in **Figure 3**, is clayey soil by replicating the same density and water content of prototype in laboratory. The properties of the used clayey soil was given in **Table 2**. The coarse-grained soil was air-dried sandy soil has a moisture content of 0.49%, the properties are shown in **Table 3**.

Table 2: property of the clayey soil

Parameters	Value	ASTM NO.
Soil classification according to USCS	CL	D2487-17
Dry unit weight (kN/m^3)	15.61	
Water content (%)	19.86	
Specific gravity	2.69	D854-02
compression Index	0.2647	D4546 -14
Swelling Index	0.02348	
Initial void ratio (e_i)	0.9918	D7263 – 09
Cohesive Strength (kPa)	71.83	
Frictional angle (°)	30.57	
Liquid limit (%)	45.5	D4318 − 10
Plastic limit (%)	25.7	
Plasticity index (%)	19.8	
Unconfined compression strength (kPa)	225.48	
Unconfined shear strength (kPa)	112.74	
modulus of elasticity (kPa)	153736	
Poisson's ratio	0.509	
Optimum moisture content (%)	20.9	D698 -12
$\gamma_{dry(max)}$ kN/m^3	15.88	

Table 3: property of the sandy soil

Density	Parameter	Values	ASTM No.
Grain size distribution	Specific gravity, Gs	2.66	D854
	D_{10} (mm)	0.2	D422
	D_{30} (mm)	0.39	
	D_{60} (mm)	0.77	
	Coefficient of uniformity, Cu	3.85	
	Coefficient of curvature, Cc	0.987	
	classification according to USCS	SP	D2487

compactness	Minimum unit weight (kN/m^3)	15.33	D4254
	Maximum unit weight (kN/m^3)	17.89	D4253
Low density	Relative density (%)	15.2	
	Total unit weight (kN/m^3)	15.67	
	The angle of internal friction (Ø), deg.	28.73	D3080
	Void ratio	0.67	
Medium density	Relative density (%)	46.16	
	Total unit weight (kN/m^3)	16.42	
	The angle of internal friction (Ø), deg.	31.84	D3080
	Void ratio	0.597	
High density	Relative density (%)	78.05	
	Total unit weight (kN/m^3)	17.26	
	The angle of internal friction (Ø), deg.	36.33	D3080
	Void ratio	0.519	

2.3 Model test schemes

A total of 10 trials were performed, one trial on the clayey soil and another 9 trials on the sandy soil. The spacing between piles was kept invariable equal to 4 mm, for the clayey soil used 1/3 as embedment ratio (ER),which is mean that 1/3 of pile length embedded in the soil and remained 2/3 is retained the excavated soil. For the sandy soil three embedment ratios were used by 1/3, 1/2, and 2/3 for each state of the low, medium, and high relative density.

The surcharge was applied to the model on the (0.3 * 0.15) m, 2 cm behind the pile's inner face. Piles are connected by the pile cap at the top. Using a plastic sheet by thickness of 8 mm on the outer face of the pile and a sponge on the edge to prevent extrude of sand between the pile spacings, and six dial gauges (three above and three in the middle) were used and fixed to measure the top and bottom lateral displacements. The model is illustrated in **Figure 5**.

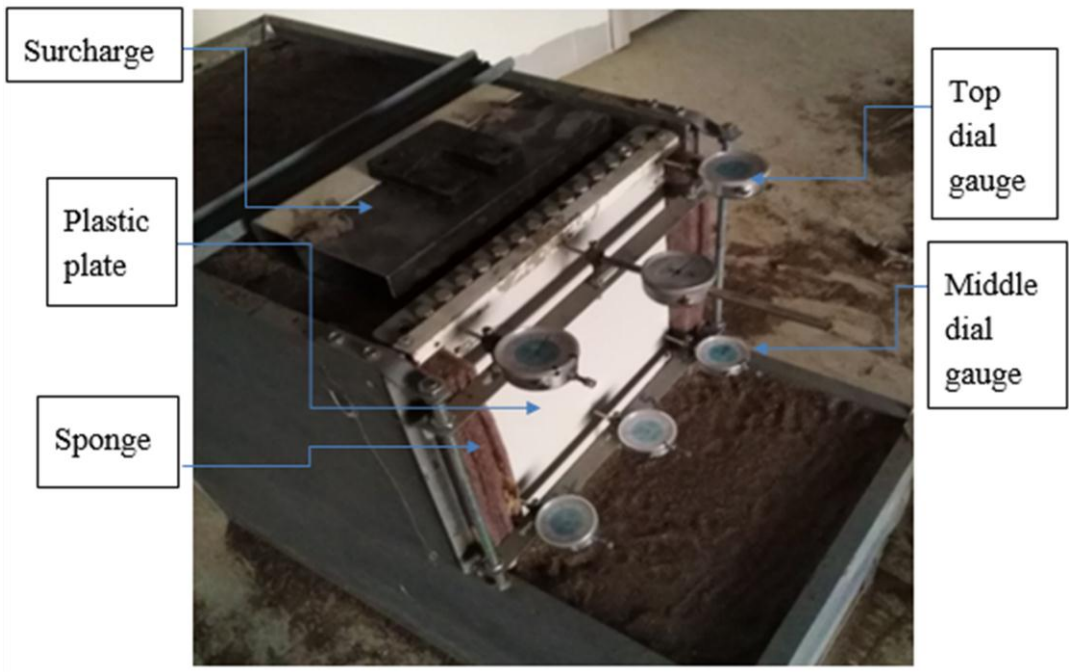

Figure 5: Experimental model.

Surcharge applied on a rectangular shape plate for these rectangular types of stress used Fadum chart for calculation vertical stress along pile depth by Eq. (1) below (Das, 2010).

$$\Delta\sigma = q\, I_\sigma \qquad ...(1)$$

Which: $\Delta\sigma$= total stress increases due to the loaded area (kPa), q= applied surcharge pressure (kPa), and I_σ= vertical influence value.

For calculation of the lateral stress along the pile , Eq. (2) was used.

$$\sigma_h = K\, \sigma_v \qquad \ldots(2)$$

Which: σ_h= total lateral stress on pile, K= lateral earth pressure coefficient (used $K_a$for the active side and K_p for the passive side), and σ_v= total vertical stress (surcharge+ overburden pressure due to soil).

The typical example for lateral stress on the critical pile is by applying 10.34 kPa surcharge stress for medium sand at embedment ratio 1/3 shown in **Figures 6 and 7** for the active and passive sides, respectively. Pile center of rotation from top at applying 10.34 kPa surcharge is equal to 535.3 mm. This rotation lead to reversing pressure in the active and passive sides, which cause to changing active pressure to passive pressure and inversely is true(Atkinson, 2007).

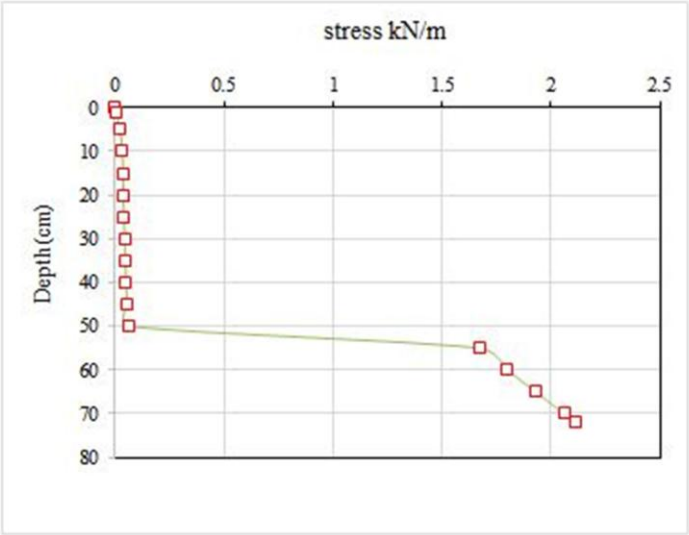

Figure 6: Lateral stress for critical pile at active side for medium sand

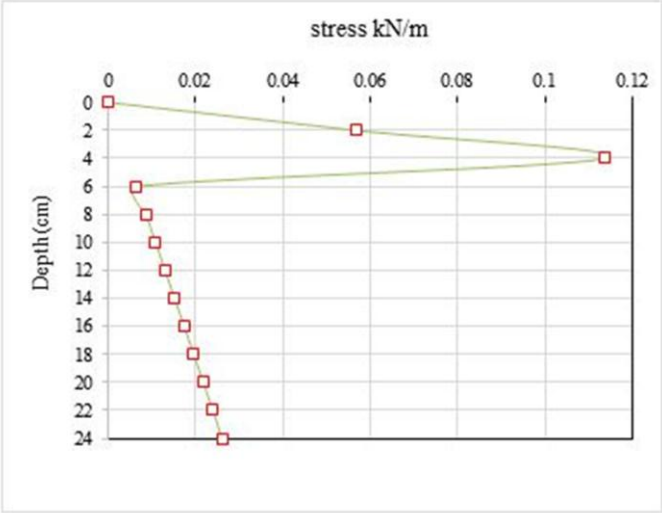

Figure 7: Lateral stress for critical pile for the passive side for the medium sand.

The lateral displacement of the pile head and pile tips were obtained based on the physical scaling model test in Section 2.1. The experimental results of contiguous piles for 720 mm length of pile, based on **Table 1** determined the allowable lateral displacements, the lateral displacement for sand in loose, medium, and dense states equal to 1.44, 1.08, and 0.72 mm respectively. For the stiff clay equal to 7.2 mm. To determine the effect of density and embedment ratio (ER), selected the allowable elastic displacement (AED) of 6% of pile diameter equals to1.2mm for all cases (Shirato et al., 2009),

The result of the test for the clayey soil is shown in **Figures 8 and 9**. It is obvious that the maximum lateral displacement by applying 125kPa surcharge is less than zero (negative), the negative displacement is due to shrinkage in the soil that causes to move soil backward. Clays are susceptible to some shrinkage and swelling due to changes in moisture content. Clayey soil has high resistance to lateral displacement due to having cohesion in the particles, it is indicated that the cohesive between the clayey soil and the pile surface is greater than the lateral load require to cause displacement of the piles forward in the active case of lateral pressure, it means that the soil pressure still in the rest state, the negative displacement of the pile are not due to passive pressure of the soil, however, the value of equation ($-2C\sqrt{k_a}$) is equal to 77.46 kPa (by using Coulomb'S earth pressure theory for calculation of ka), that is greater than the maximum lateral stress produced on the critical pile by applying 125 kPa surcharge pressure which is equal to 12.17 kPa. While backward movement of the piles was due to the shrinkage characteristics of clayey soil. In this case, the crack will not occur from the top of interaction surface of soil and piles, that can be determined by the equation after the development of tensile cracks, $z_o = \frac{2C}{\gamma\sqrt{k_a}}$, where: z_o = depth at which the active pressure becomes zero. C= soil cohesion. γ = bulk unit weight. k_a = active lateral earth pressure coefficient.

Test results for sandy soil are shown in **Figure 10 to 15**, for various densities; loose, medium, and dense states. In the loose state which is shown in **Figure 10**, the pile head displacement passed the AED for ER of 0.333 and 0.5 without applying surcharge which is equal to 24.5mm, and 4mm respectively. While for the medium state which is shown in **Figure 12**, only at ER=0.333 the pile head displacement goes beyond the AED after applying overburden pressure which reached to 3.1mm, that means that medium state more stable than the loose state at overburden pressure without applying the surcharge. This behavior can be interpreted such that, with increasing density of sandy soil the angle of internal friction (Ø) increases **Table 3**, consequently the lateral pressure decreases and the wall be in a more stable state.

For the dense states, the pile head displacements are shown in **Figure 14**, at the ER=0.333 the pile head displacement decreases to 2.5mm despite of passed the AED. The experimental test results proved that the ER of 0.333 is not acceptable in all loose, medium, and dense states. And for the loose state, the ER=0.5 is also unacceptable. The result revealed that density is an important parameter that has a significant effect on lateral displacement, which revealed that with increasing density the lateral displacement decreases obviously, the reason for that is the increasing Ø, as a result, decreasing lateral pressures. Unfortunately, there are no researches in the literature that investigate the effect of density on the contiguous pile to compare our results.

The effect of ER in each state has a considerable effect to resist lateral displacements which are shown in **Figure 12 to 17**. These figures revealed that with increasing ER the slope of the curve is increasing, which means that the piles' ability to resist lateral load significantly increased and the cutting surface will be more stable. Similar behavior was reported by Ye et al. (2020) .

For loose sand, the lateral displacement at ER=1/3 was 6 and 33.7 times more than ER=1/2 and ER=2/3 respectively. While for the medium sand, the lateral displacement at ER=1/3 was 12 and 26 times more than ER=1/2 and ER=2/3 respectively, however, for dense sand the lateral displacement at ER=1/3 was 12 and 42 times more than ER=1/2 and ER=2/3 respectively.

The result revealed that the ER has a higher effect on lateral displacement. which by increasing ER the lateral displacement decreases obviously. Al-Neami et al. (2021) performed research to study the effect of ER on the response of lateral load of single and group piles, they concluded that when the ER increased, the ultimate lateral load is also increased.

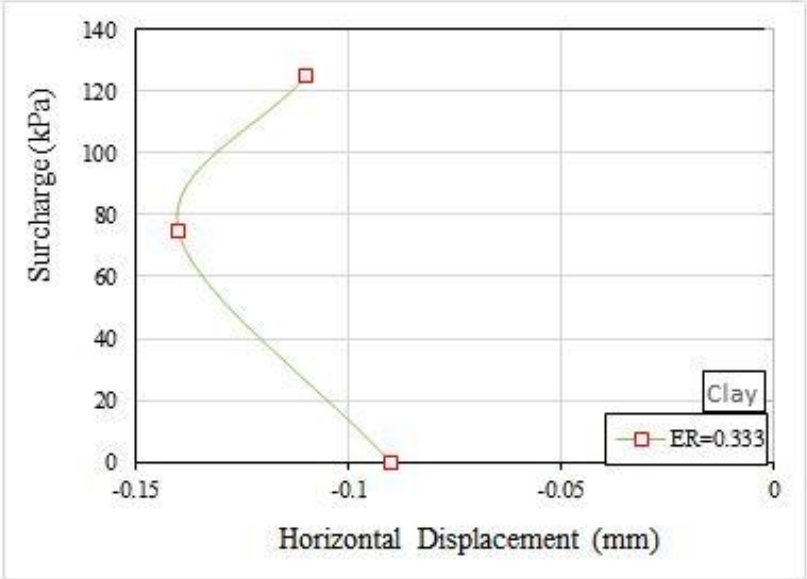

Figure 8: Top pile displacement for clay

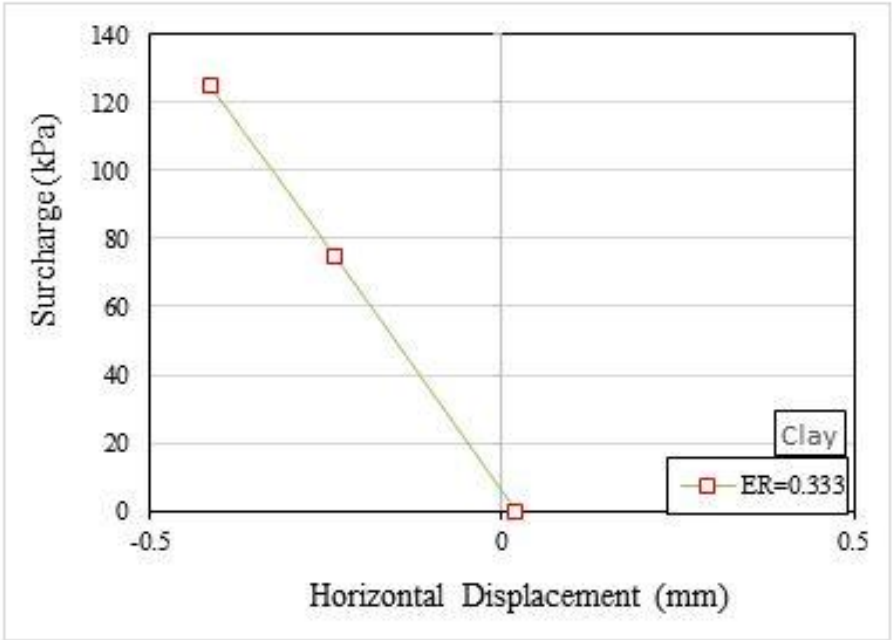

Figure 9: Tip pile displacement for clay

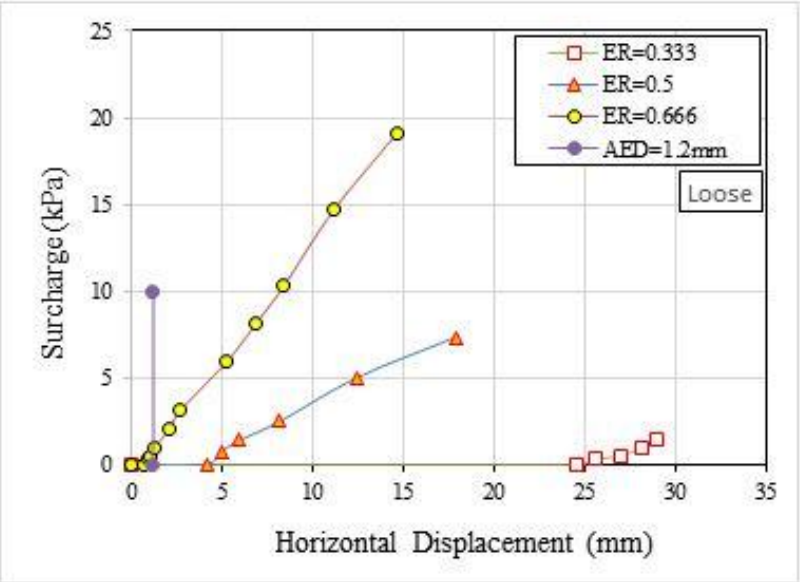

Figure 10: Top pile displacement for loose sand

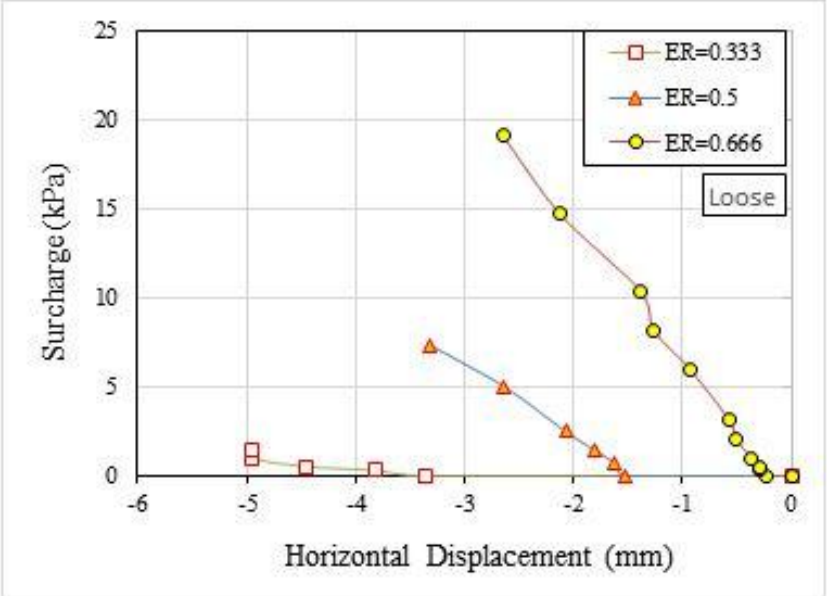

Figure 11: Tip pile displacement for loose sand

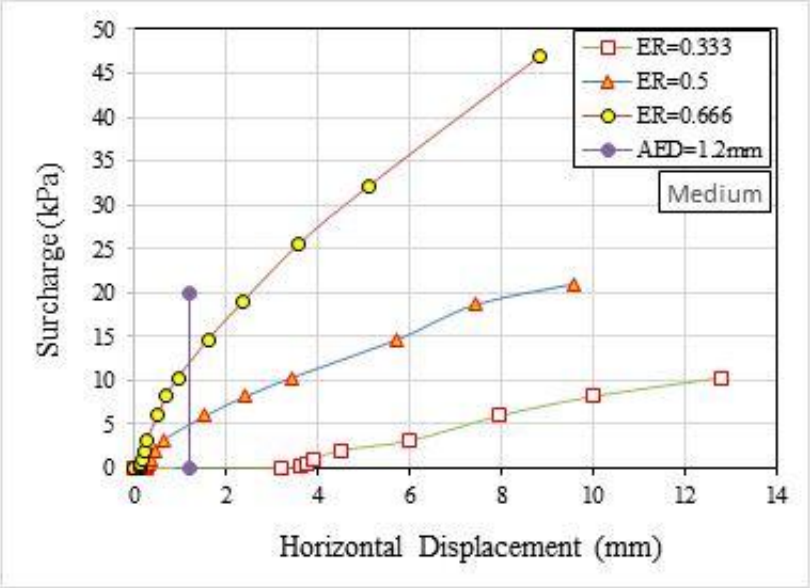

Figure 12: Top pile displacement for medium sand

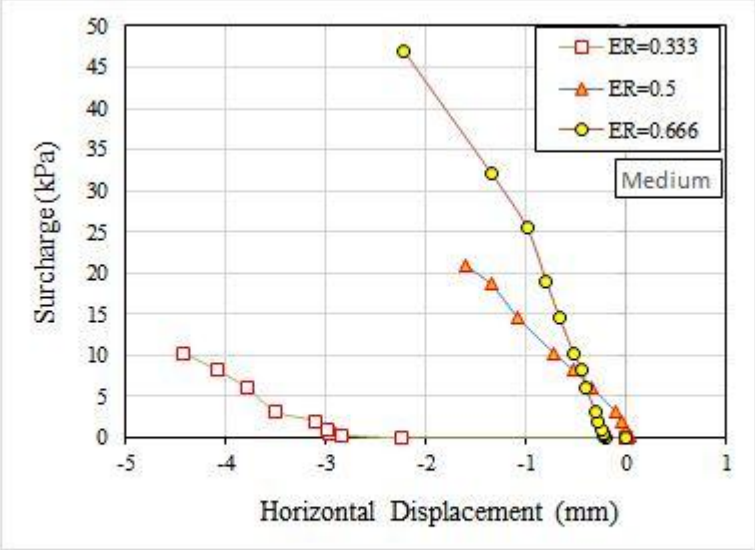

Figure 13: Tip pile displacement for medium sand

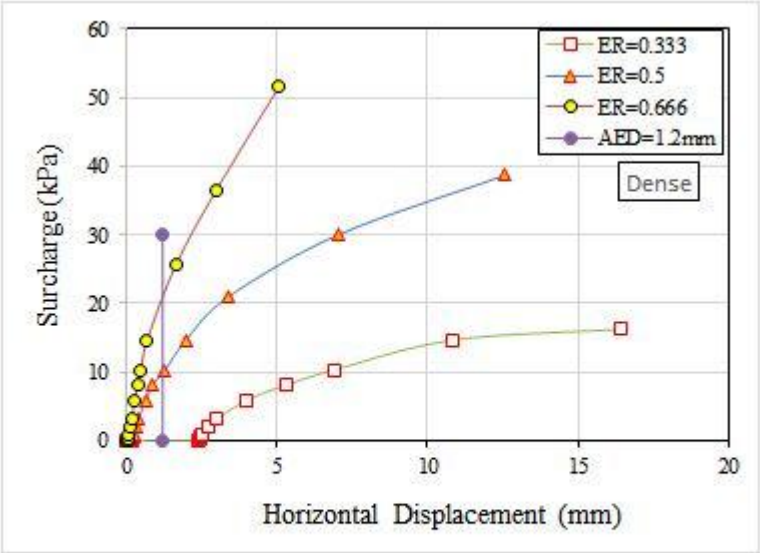

Figure 14: Top pile displacement for Dense sand

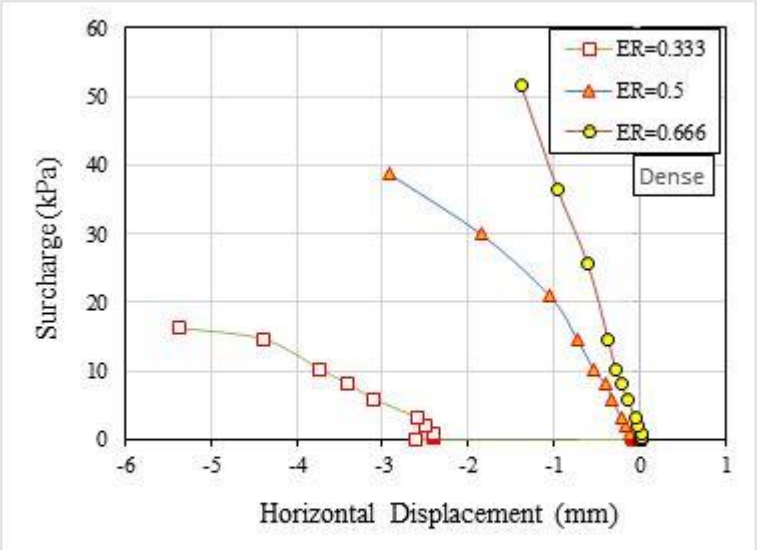

Figure 15: Tip pile displacement for Dense sand

4. CONCLUSIONS

In this study, from the experimental model about anti-slide piles on two different types of soil the following conclusion was drawn:

1) The clayey soil has a higher resistance to lateral displacement due to the cohesion between particles because no contract exists between the soil and the wall up to a depth of $z_o = \frac{2C}{\gamma\sqrt{k_a}}$ after the development of tensile cracks

2) Embedment ratio is an important parameter that affects lateral displacement, with increasing ER the lateral displacement decrease.

3) The density has a higher effect on the lateral displacement. which by increasing relative density the lateral displacement decreases obviously.

4) Due to the incoherent properties of sandy soils, its particles extrude through the spacing between the piles which requires covering these spaces.

6. References

AIMIN, H., JUNHUA, X. & GUOXIONG, M. 2006. Behavior of soil arching between passive piles and effects parameters study. *工程地质学报*, 14**,** 111-116.

AKRAWI, N. S. & AHMED, S. A. 2019. A Mathematical Model for Prediction the Embedment Depth of the Contiguous Piles Used in the Interchange of Zakho Entrance. *Polytechnic Journal*, 9**,** 119-124.

AL-NEAMI, M. A., AL-DAHLAKI, M. H., CHALOB, A. H. J. E. & JOURNAL, T. 2021. Effect of Embedment and Spacing Ratios on the Response of Lateral Load of Single and Group Piles. 39**,** 1144-1152.

ATKINSON, J. 2007. The mechanics of soils and foundations.

BROMS, B. B. 1964. Lateral resistance of piles in cohesive soils. *Journal of the soil mechanics and foundations division*, 90**,** 27-63.

BROMS, B. B. J. J. O. T. S. M. & DIVISION, F. 1964. Lateral resistance of piles in cohesionless soils. 90**,** 123-156.

CAI, F. & UGAI, K. 2011. A subgrade reaction solution for piles to stabilise landslides. *Geotechnique*, 61**,** 143-151.

CHIK, Z. H., ABBAS, J. M., TAHA, M. R. & SHAFIQU, Q. S. M. J. E. J. O. S. R. 2009. Lateral behavior of single pile in cohesionless soil subjected to both vertical and horizontal loads. 29**,** 194-205.

CLAYTON, C. R., WOODS, R. I. & MILITITSKY, J. 2014. *Earth pressure and earth-retaining structures*, CRC press.

DAS, B. M. 2010. *Geotechnical engineering handbook*, J. Ross publishing.

GODAVARTHI, V. R., MALLAVALLI, D., PEDDI, R., KATRAGADDA, N. & MULPURU, P. 2011. Contiguous pile wall as a deep excavation supporting system. *Leonardo Electronic Journal of Practices and Technologies*, 19**,** 144-160.

HASSIOTIS, S., CHAMEAU, J. & GUNARATNE, M. 1997. Design method for stabilization of slopes with piles. *Journal of Geotechnical and Geoenvironmental Engineering*, 123**,** 314-323.

JOHARI, A. & NAKHAEE, M. Maximum lateral displacement prediction of bored pile wall in granular soil using Gene Expression Programming. National Congress on Civil Engineering, University of Sistan and Baluchestan, Zahedan, Iran, 2013.

KAHYAOGLU, M. R., IMANÇLI, G., ÖNAL, O. & KAYALAR, A. S. 2012. Numerical analyses of piles subjected to lateral soil movement. *KSCE Journal of Civil Engineering*, 16**,** 562-570.

KANAGASABAI, S., SMETHURST, J. & POWRIE, W. 2011. Three-dimensional numerical modelling of discrete piles used to stabilize landslides. *Canadian Geotechnical Journal*, 48**,** 1393-1411.

KEAWSAWASVONG, S., UKRITCHON, B. J. C. & GEOTECHNICS 2017. Undrained limiting pressure behind soil gaps in contiguous pile walls. 83**,** 152-158.

KOURKOULIS, R., GELAGOTI, F., ANASTASOPOULOS, I. & GAZETAS, G. 2012. Hybrid method for analysis and design of slope stabilizing piles. *Journal of Geotechnical and Geoenvironmental Engineering*, 138**,** 1-14.

LI, C., TANG, H., HU, X. & WANG, L. J. K. J. O. C. E. 2013. Numerical modelling study of the load sharing law of anti-sliding piles based on the soil arching effect for Erliban landslide, China. 17**,** 1251-1262.

LI, H., TONG, L., LIU, S., LIU, H. & ZHANG, M. 2018. Construction and verification of a unified p–y curve for laterally loaded piles. *Bulletin of Engineering Geology and the Environment*, 77**,** 987-997.

LIU, M., WANG, H. & ZHANG, H. Analysis of pile spacing considering end-bearing soil arching and friction soil arching. E3S Web of Conferences, 2020. EDP Sciences, 01014.

LIU, Q., LI, D.-Y., LIU, Z.-X. & LIU, J. 2011. Numerical analysis of influence factors on soil arching effect between anti-sliding piles under horizontal pushing loads. *Journal of Central South University (Science and Technology)*, 42**,** 2071-2077.

LIU, X.-R., KOU, M.-M., FENG, H. & ZHOU, Y. 2018. Experimental and numerical studies on the deformation response and retaining mechanism of h-type anti-sliding piles in clay landslide. *Environmental earth sciences*, 77**,** 1-14.

MONEY, B., HODGSON, G. & HODGSON, G. J. 1996. *Manual of Contract Documents for Highway Works: A User's Guide and Commentary: 1993/1994 Amendments*, Thomas Telford.

MURARO, S., MADASCHI, A. & GAJO, A. 2014. On the reliability of 3D numerical analyses on passive piles used for slope stabilisation in frictional soils. *Géotechnique*, 64**,** 486-492.

OU, C.-Y. 2014. *Deep excavation: Theory and practice*, Crc Press.

POULOS, H. G. 1995. Design of reinforcing piles to increase slope stability. *Canadian Geotechnical Journal*, 32**,** 808-818.

PRAKASH, S. & SHARMA, H. D. 1991. *Pile foundations in engineering practice*, John Wiley & Sons.

RATHOD, D., MUTHUKKUMARAN, K. & SITHARAM, T. 2018. Effect of slope on p-y curves for laterally loaded piles in soft clay. *Geotechnical and Geological Engineering*, 36**,** 1509-1524.

RP, A. J. A. R. G. 2011. Geotechnical and foundation design considerations.

SHIRATO, M., KOHNO, T. & NAKATANI, S. Geotechnical criteria for serviceability limit state of horizontally loaded deep foundations. Proc. of the Second International Symposium on Geotechnical Risk and Safety, 2009. 119-126.

SHOOSHPASHA, I. & AMIRDEHI, H. 2015. Evaluating the stability of slope reinforced with one row of free head piles. *Arabian Journal of Geosciences*, 8**,** 2131-2141.

TANG, H., HU, X., XU, C., LI, C., YONG, R. & WANG, L. J. E. G. 2014. A novel approach for determining landslide pushing force based on landslide-pile interactions. 182**,** 15-24.

WOOD, D. M. 2017. *Geotechnical Modelling*, CRC Press.

XING, W., XIANGJUN, P. & YUNPENG, L. 2013. Stress characteristics and soil arch effect analysis of anti-

sliding piles with special cross-section. ***工程地质学报,*** 21**,** 797-803.

YE, J., WANG, C., HUANG, W., ZHANG, J. & ZHOU, X. J. T. V. 2020. Effect of inclination angle on the response of double-row retaining piles: experimental and numerical investigation. 27**,** 1150-1159.